MECHANICAL AND DURABILITY PERFORMANCE OF HIGH-STRENGTH COCRETE FOR PRESTRESSED CONCRETE BRIDGE APPLICATION

Haimoon Cheong, Tae-Song Ahn and Young-Soo Yoon*,
Expressway & Transportation Research Institute., Korea Expressway Corporation, 50-5, Sancheok-ri, dongtan-myeon, hwaseong, Gyeonggi, 445-812, Korea. haimoon@ex.co.kr
***Dept. of Civil and Environmental Engineering, Korea University.,**
1, 5-ga, Anam-dong, Seongbuk-gu, Seoul, 136-701, Korea

ABSTRACT

Several tests, focusing on the effects of the type and composition of cementitious materials (ordinary Portland cement, fly ash, slag, low-heat cement, and their combinations), mechanical properties and durability of high-strength concrete, were performed to provide experimental data for application of high-strength concrete to prestressed bridges. Firstly, mix proportions were designed based on a number of trial mixes, taking into account their applicability to prestressed bridges. Mechanical properties, such as compressive strength, modulus of elasticity, splitting tensile strength and flexural strength, were determined. Durability related properties, such as hydration temperature, resistance to chloride-ion penetration, resistance to freezing-thawing, autogenous and drying shrinkages and creep were also determined. The effects of cementitious materials on high-strength concrete properties have been demonstrated.

INTRODUCTION

Currently, demand for high-strength concrete (HSC) for prestressed bridges is gradually increasing as using HSC allows engineers to design bridges with longer spans for a given girder cross section, thus reducing the number of girders per span by increasing girder spacing, that can lead to substantial costs savings for bridges (Russell 1994; Hueste et al. 2004). The definition of HSC continues to change as advances in concrete technology make it easier to achieve increasingly higher strength using conventional construction practices. In the late 1970s, 42 MPa concrete was looked upon as being high strength, but more recently 60 MPa has been considered the lower boundary for HSC (FIP/CEB 1990). The rapid increase in available concrete strength is due principally to the development of superplasticizers and the application of mineral admixtures.

However, design provisions for prestressed concrete members under current codes are primarily based on empirical relationships of the mechanical properties developed testing normal strength concrete (NSC) (Hueste et al. 2004). Extrapolation of these empirical equations to materials of higher strength, with different microstructures is not justified and may not be conservative. In contrast, equations may be too conservative, so that the advantages of using HSC are not fully realized. In addition, there is a lack of experimental data on the relative effects of these cementitious materials on HSC for use in prestressed bridges.

The objective of this study is to obtain information on mix proportions, mechanical properties and durability of HSC for use in prestressed bridges. Basically, in mix design, the concrete compressive strength at an early age when prestressing forces are introduced to prestressed concrete members, and the slump which is proper for pumping of concrete, were considered to make a concrete suitable for prestressed concrete bridges. In addition to compressive strength and slump, air content was considered to enhance durability of prestressed concrete bridges under severe environments. The main parameters investigated were type and composition of cementitious materials, those being, ordinary Portland cement (OPC), fly ash (FA), ground granulated blast furnace slag (BS) and low-heat

cement (LHC). Experimental tests conducted on materials' mechanical properties including compressive strength, modulus of elasticity, splitting tensile strength and flexural strength. Tests for chloride-ion penetration, freezing-thawing, combined deterioration and hydration temperature were also performed to investigate the durability of the developed HSC. Furthermore, time-dependent deformation, such as creep, drying and autogenous shrinkage, which is a particularly important factor in design and construction of prestressed concrete bridges, was tested and analyzed.

MATERIALS

Cementitious materials used in tests were OPC, FA, BS and LHC, and their chemical composition and physical properties are given in Table 1. The coarse aggregate used was crushed granite, with a specific gravity, fineness modulus and maximum particle size of 2.63, 6.59 and 20 mm, respectively. The fine aggregate was quartz sand with a specific gravity and fineness modulus of 2.59 and 2.84, respectively. The superplasticizer was a polynaphthalene sulfonated-based admixture, with 40% solids in a dark brown solution with a specific gravity of 1.22. A Vinsol resin-type air-entraining admixture was used.

Table 1 Physical properties and chemical composition of binders

	OPC	FA	BS	LHC
SiO_2	21.3	52.8	34.3	25.3
Al_2O_3	4.7	22.5	12.7	3.1
Fe_2O_3	3.1	13.4	0.5	3.6
CaO	63.1	4.1	41.3	62.5
MgO	2.9	0.8	5.93	2.0
SO_3	2.2	0.4	2.53	2.3
Loss on ignition	0.8	3.8	0.48	0.9
C_3S	59.8	-	-	31
C_2S	13.7	-	-	48
C_3A	5.1	-	-	2
C_4AF	9.3	-	-	11
Specific gravity	3.15	2.13	2.91	3.19
Fineness (m^2/kg)	341	348	453	357

MIX PROPORTIONS

For the application of HSC to prestressed bridges, all mixtures were proportioned to give the 28-day design strength of 60 MPa. At the same time, a 3-day compressive strength of 30 MPa target was set up for all mixtures, as the strength of concrete at an early age is considerably significant due to requirements of the early transfer of prestress. The water to cementitious materials ratio (w/b) was kept at 0.28 for all mixtures. With recent advances in concrete workability, the slump height is often so large that it is difficult to distinguish among different batches. The ''slump flow'', or diameter of the base of the slumped material, is often used instead of the height measurement (Saak et al. 2004). Bridge concrete may lose a certain amount of slump due to pumping of the concrete, which is statistically significant (Yazdani et al. 2000). Therefore, the amount of superplasticizer was adjusted to obtain the desired level of workability maintaining a slump and slump flow of 230±25 and 500±50 mm, respectively. To enable the development of durable concrete for prestressed concrete bridges, air content of all mixtures was kept at 5.5±1.0% by adjusting the dosage of the air-entraining admixture.
Based on the type and composition of cementitious material, mixtures were designated as OPC, FA10, FA20, BS30, BS50, FA15BS35 and LHC. The number in the designation represents the percentage

mass of the total cementitious materials; for example, Mix FA15BS35 contained 15 and 35% fly ash and slag, respectively. Mix LHC contained no OPC, but 100% low-heat cement. Mix proportions, as shown in Table 2, were determined after testing different trial mixes at least 240 times.

Table 2 Mix proportions (kg/m^3)

Mix designation	W/b	Water	Cement	Fly ash	Slag	Fine aggregate	Coarse aggregate
OPC	0.28	170	607	-	-	676	910
FA10	0.28	170	546	61	-	667	898
FA20	0.28	170	486	121	-	658	885
BS30	0.28	170	425	-	182	668	900
BS50	0.28	170	304	-	304	663	892
FA15BS35	0.28	170	304	91	213	653	879
LHC	0.28	170	607*	-	-	676	910

EXPERIMENTAL PROGRAM

After casting, the specimens were covered with plastic sheets and left in the casting room for 24 hours at 20±2 °C, and then they were demolded and stored in water at 20±3 °C until tested.

The concrete hydration temperature was measured on 64ℓ (400 × 400 × 400 mm) specimens cast in a semi-adiabatic cube made of Styrofoam. Thermocouples were placed in the center of the specimens and connected to a maturity meter.

Compressive strength and modulus of elasticity were tested on 100 × 200 mm cylinders at 3, 7, 28 and 56 days after casting, according to ASTM C 39 and ASTM C 469, respectively. Splitting tensile strength was evaluated using 100 × 200 mm cylinders at 7, 28 and 56 days, according to ASTM C 496. The flexural strength of prism specimens (150 × 150 × 550 mm) was determined at 7, 28 and 56 days, according to ASTM C 78.

Resistance of concrete to chloride ion penetration, measured in terms of the charge passed through the concrete was determined on 50 mm thick slices of 100 mm diameter cylinders at the 28th day. The concrete disc was placed between two solutions, with one end of the disc in contact with a 0.3 N NaOH acolyte solution and the other in contact with a 3 % NaCl catholyte solution. After exposure, the concrete disc was split longitudinally, and the depth to which chloride has penetrated into the disc was determined by applying silver nitrate solution to the freshly split surface, which colored the areas containing chloride ions white. The diffusion coefficient was then calculated from Eq. (1).

$$D = \frac{RT}{zFE} \cdot \frac{x_d - \alpha\sqrt{x_d}}{t} \quad (1)$$

$$E = \frac{U - 2}{L} \quad (2)$$

$$\alpha = 2\sqrt{\frac{RT}{zFE}} \cdot erf^{-1}\left(1 - \frac{2c_d}{c_0}\right) \quad (1b)$$

where D=non-steady-state migration coefficient (m^2/sec), z=absolute value of ion valence (for chloride z=1), F=faraday constant (F=9.648×10^4) (J/V·mol), U=absolute value of the applied voltage (V), R=gas constant (R=8.314) (J/K·mol), T=average value of the initial and final temperatures in the anolyte solution (K), L=thickness of the specimen (m), x_d=average value of the penetration depths (m), t=test duration (sec), erf=error function, c_d=chloride concentration at which the color changes (c_d≈0.07

N), and c_0=chloride concentration in the catholyte solution (c_0≈2 N).

Resistance to freezing and thawing was measured on 100 × 100 × 400 mm concrete prisms, according to ASTM C 666, Procedure A. To examine how combinations of deicer salt application and freezing-thawing cycles affected deterioration of concrete, concrete exposed to freeze–thaw cycles in fresh water or in 10 % $CaCl_2$ solution was tested. The specimen weight and fundamental transverse frequency were monitored and measured according to ASTM C 215, at intervals of 30 cycles.

Autogenous shrinkage was measured on 10 × 100 × 400 mm concrete prisms immediately after casting for periods of up to 28 days by means of an embedded gage. A thermocouple was also inserted into the middle of each specimen to monitor temperature changes. At an age of 24 hours, the specimens were promptly demolded, and all surfaces sealed with aluminum adhesive tape. Specimens were then placed vertically in a control room at 23±1 °C and 60±3 % relative humidity. According to ASTM C 157, the drying shrinkage was also measured on specimens having the same dimensions, materials and air conditions as those of the specimens used in the autogenous shrinkage test for the same period.

To cope with the difficulties in isolating strains due to concrete shrinkage from those caused by creep, simultaneous creep and concrete shrinkage tests were performed. Strains caused by creep were measured on 150 × 300 mm cylinders by means of an embedded gage, according to ASTM C 512, and concrete shrinkage strains were measured on unloaded specimens having the same dimensions and materials as those loaded. The load was applied at the 3rd day to find out if prestressing forces could be applied to concrete members at an early age. The creep test was carried out for 90 days.

RESULTS AND DISCUSSION

Hydration Temperature

Hydration temperature at an early age is shown in Fig. 1. The decrease in hydration temperature depends not only on the rate of replacement, but also on the type of cementitious materials incorporated. For example, for FA10, FA20 and BS50, the highest temperature increases were 1.8, 2.7 and 4.9 °C lower than that of OPC, respectively. However, the highest temperature increase of BS30 was the same as that of OPC. As for the ternary mixture, FA15BS35, the highest temperature increase was much lower than that of OPC or specimens made with single mineral admixtures. LHC had the smallest temperature increase, which was 12.8 °C lower than that of OPC. All specimens had similar arrival times for the highest temperature increase. This phenomenon could be explained by noting the high volume of cementitious materials diluted on cement particles at an early age, resulting in an improvement of the hydration environment of the cement. As a result, for HSC with a low w/b, the cement hydration process was accelerated.

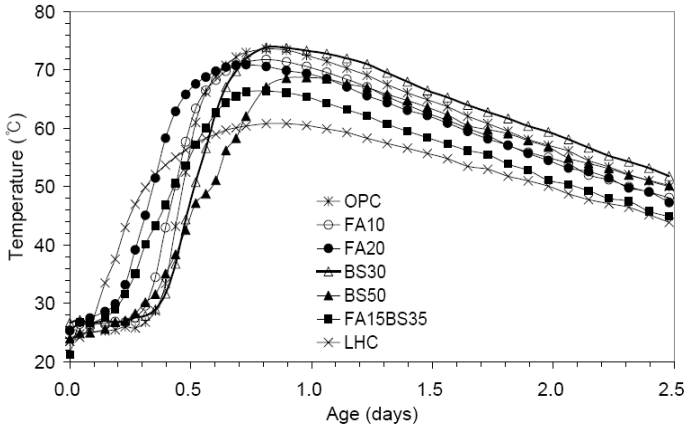

Fig. 1 Variation of temperature in the concretes

Compressive Strength

Strength developed by the concrete samples at 3, 7, 28 and 56 days is shown in Fig. 2. As expected, replacement of cement by the weight of mineral admixtures resulted in decreased compressive strengths at an early age compared with the strength of OPC and LHC. Especially, for concretes having a large proportion of mineral admixtures, such as FA20, BS50 and FA15BS35, the target strength value of 30 MPa at the 3rd day was not achieved. At the 7th day; however, compressive strengths of all the concrete samples exceeded 30 MPa, and at the 28th day, the design strength of 60 MPa was achieved for all mixes, with the exception of FA20. The addition of fly ash caused a considerable reduction in compressive strength, which was reduced by as much as 35% on the addition of 20% fly ash at the 28th day. Because of the slow pozzolanic reactions of fly ash, continuous wet curing and favorable curing temperatures are required for the proper development of strength. It should be noted that fly ash has been used in the production of HSC when cured for a long period of time (Toutanji et al. 2004). Although concretes incorporating fly ash, such as FA10, FA20 and FA15BS35, developed lower strengths than OPC, their rate of strength increase after 28 days was higher than the other concretes. Concretes incorporating slag, such as BS30 and BS50, had the highest strengths at the 28th and 56th days.

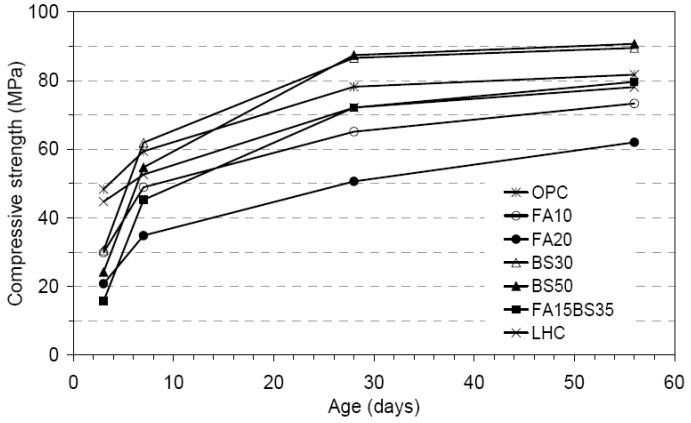

Fig. 2 The development of compressive strength

Modulus of elasticity

The modulus of elasticity of the concretes determined at the 3rd, 7th, 28th and 56th days are shown in Table 3. To evaluate the accuracy of equations; ACI 318-05 and ACI 363R-92, in predicting the modulus of elasticity when supplementary cementitious materials are added to the concrete, the modulus of elasticity from the test results was compared with those obtained using these equations, as shown in Fig. 3. The prediction equations, ACI 318-05 and ACI 363R-92, are given by Eq. (3) and (4), respectively.

$$E = 4700\sqrt{f_c^{'}} \quad \text{(MPa)} \tag{3}$$

$$E_c = 3320\sqrt{f_c^{'}} + 6900 \quad \text{(MPa)} \quad \text{for} \quad 21MPa \le f_c^{'} \le 83MPa \tag{4}$$

Where $f_c^{'}$ is the specified compressive strength of concrete in MPa.

As shown in Fig. 3, ACI 363R-92 has a better prediction modulus values than ACI 318-05. This graph shows that the prediction equation of ACI 363R-92 can be used to predict the modulus values for HSC incorporating supplementary cementitious materials.

The initial modulus of elasticity is important to the precast prestressed industry for investigating certain effects, such as elastic shortening (Mokhtarzadeh et al. 1995). Results obtained from this study indicate that the 3rd day modulus of elasticity measured on concretes incorporating mineral admixtures was less than 70% of that obtained at the 28th day, while those of OPC and LHC were

approximately 97 and 73.3% of their 28th day values, respectively. At the 7th day, however, the elastic moduli of all types of concrete were over 80% of those obtained at the 28th day.

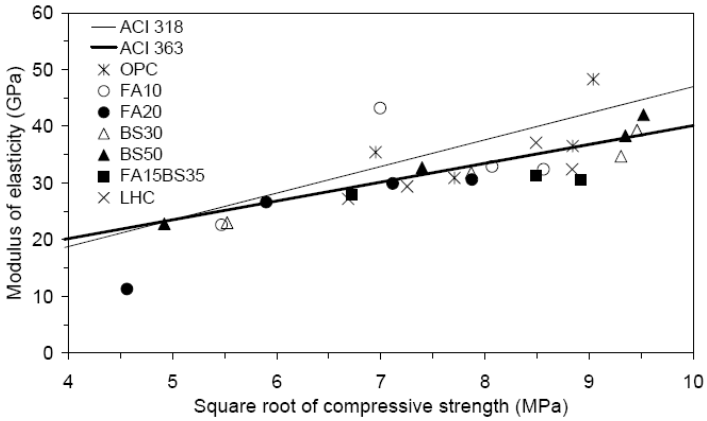

Fig. 3 Comparison of the ACI equations and test results for the elastic modulus

Splitting tensile and flexural strength

Table 3 shows the test results of the splitting tensile and flexural strength. The tensile to compressive strength ratio of concrete depends on the general level of the compressive strength; the higher the compressive strength, the lower the ratio. The direct tensile to compressive strength ratio for NSC is reported to be between 8 ~ 9%, but that for HSC is decreased to be about 5% (Metha and Monteiro 1993; Neville 1995). Test results show that the splitting tensile to compressive strength ratio of all the concretes ranged from 3.9 to 9.5%, and the flexural strength was found to increase with increasing compressive strength. However, the type and composition of cementitious material showed no significant effects on the splitting tensile and flexural strength.

Table 3 Modulus of elasticity, splitting tensile and flexural strength test results

	Modulus of elasticity(GPa)				Splitting tensile strength			Flexural strength(MPa)		
Mix designation	3rd Day	7th Day	28th Day	56th Day	7th Day	28th Day	56th Day	7th Day	28th Day	56th Day
OPC	35.4	30.9	36.5	48.3	3.6	3.9	3.7	9.8	11.1	10.1
FA10	22.6	43.2	32.9	32.4	3.2	3.5	4.0	8.4	10.4	9.3
FA20	11.3	26.6	29.9	30.6	3.3	3.4	3.2	8.3	8.3	10.3
BS30	23.0	31.8	34.7	39.3	3.0	3.6	3.5	12.5	12.1	11.1
BS50	22.8	32.7	38.3	42.0	3.9	4.4	4.5	11.1	10.2	11.5
FA15BS35	10.7	27.9	31.2	30.5	3.9	4.2	5.7	8.3	10.6	10.5
LHC	27.2	29.7	37.1	32.4	3.3	3.9	4.5	6.9	9.2	9.2

Resistance to chloride-ion penetration

Results for the resistance of concrete to chloride-ion penetration are given in Fig. 4. The effect of cement replacement on the resistance to chloride-ion penetration is clearly illustrated. As the rate of replacement increases, the chloride migration coefficient decreases, as both fly ash and blast furnace slag may improve pore size distribution as well as pore shape of the concrete. FA15BS35 showed the lowest chloride-ion permeability of all the concretes tested. However, FA20 had the highest chloride migration coefficient, which was inconsistent with other results from the literature (Leng et al. 2000). At the test age, FA20 had the lowest compressive strength, that is, more pores and diffusing paths may form with the low strength, so the chloride ion diffusion coefficient may increase. Figure 5 shows the relationship between the chloride migration coefficient and compressive strength. The chloride migration coefficient decreased with increasing compressive strength, but this was not the case for LHC.

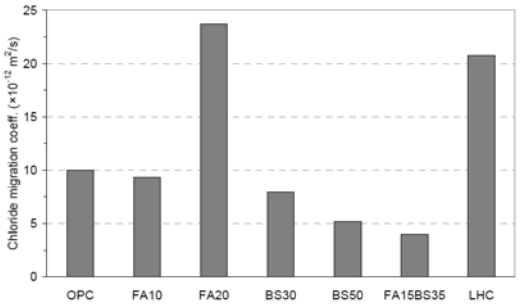

Fig. 4 Chloride migration coefficient of the concretes

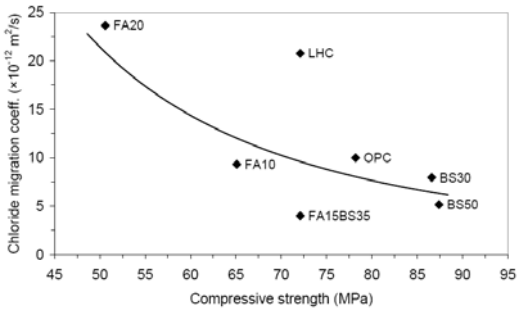

Fig. 5 Relation between the chloride migration coefficient and compressive strength

Resistance to freezing and thawing

Durability factors of the test specimens in water and $CaCl_2$ solution are plotted in Fig. 6. Due to the chamber capacity limitations for storage, BS30 was excluded from the test as other studies have shown no correlation between slag contents and durability factor (Toutanji et al. 2004). For all specimens immersed in fresh water, with the exception of FA20, calculated durability factors were over 90 after 300 cycles. As observed from the results, the greater the amount of fly ash, the lower the resistance to freeze and thaw exposure. Considering the slow pozzolanic reactions of fly ash, a curing period of only 14 days may result in decreased resistance to freezing and thawing.

In actual concrete applications, the concrete surface scales markedly when exposed to freeze–thaw cycles and de-icing salt (Mu et al. 2002). Results shown in Fig. 6 indicate that concretes subjected to freeze–thaw cycles in $CaCl_2$ solution had lower durability factors than in water, with the test results for concretes in $CaCl_2$ solution showing similar tendencies to those in water. However, for the mixes with low or no replacement rates, such as FA10, OPC and LHC, the chloride solution did not significantly affect resistance to freezing and thawing.

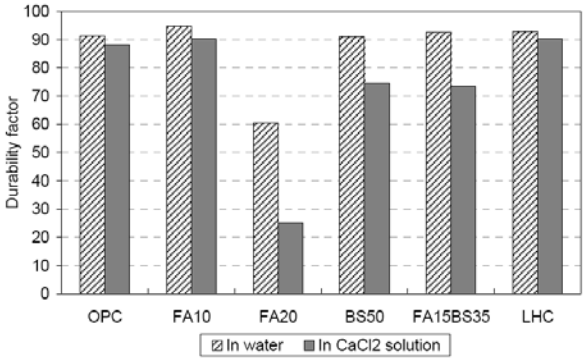

Fig. 6 Durability factor of the concretes in water and $CaCl_2$ solution

Autogenous and drying shrinkage

Although there were no differences between autogenous and drying shrinkages in relation to decreased humidity in hardened cement body, there is a difference in their mechanisms; drying shrinkage is the evaporation of water towards the outer environments; whereas, autogenous shrinkage is consumption of water due to a hydration reaction (JCI 1999). Therefore, the small amount of water used for mixing in HSC is rapidly consumed by early age hydration of the cement. This is the main reason why a large amount of autogenous shrinkage is observed with HSC. Besides w/c and cement content, various pozzolanic materials also affect the autogenous shrinkage behavior of HSC in different manners (Tazawa and Miyazawa 1995).

Figures 7 and 8 show the results of the autogenous and drying shrinkage tests, and it is evident that autogenous shrinkage increases when part of the OPC is replaced by slag. With further increases in slag content, autogenous shrinkage slightly decreases. The effect of slag in increasing autogenous

shrinkage was also observed in drying shrinkage, as shown in Fig. 8. However, contrary to the effect of the replacement rate of slag on autogenous shrinkage, dry shrinkage increases considerably with increasing slag content. The incorporation of fly ash into HSC leads to a decrease in autogenous shrinkage; the higher the fly ash content, the lower the autogenous shrinkage. However, fly ash, as with slag, helps increase drying shrinkage, as shown by Fig. 8. When both slag and fly ash are incorporated, the effect of the slag appears to dominate the shrinkage characteristic of HSC. The trend for FA15BS35 was similar in terms of both autogenous and dry shrinkages to that of concretes incorporating slag. LHC showed the least autogenous and dry shrinkages. In addition, LHC had a very low ratio of autogenous shrinkage to drying shrinkage, which was only 25.3%. The relation between the autogenous to drying shrinkage ratio at the 28th day and compressive strength is given in Fig. 9. The autogenous to drying shrinkage ratio increased with the increase of compressive strength, suggesting most of the drying shrinkage cannot be attributed to evaporation, but to autogenous shrinkage for HSC.

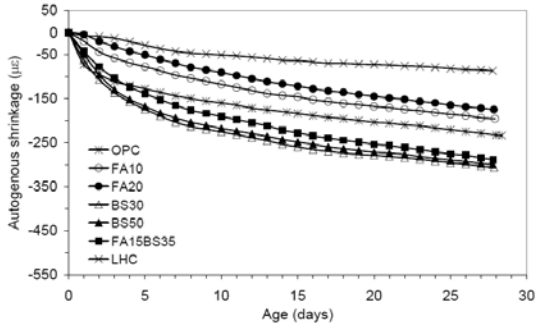

Fig. 7 Autogenous shrinkage

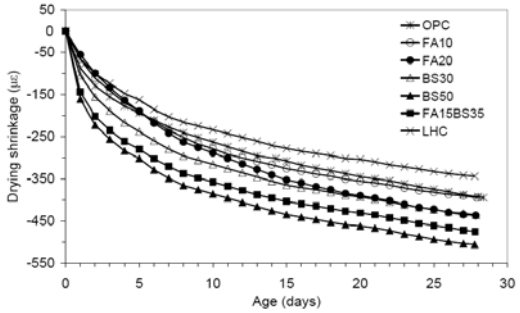

Fig. 8 Drying shrinkage

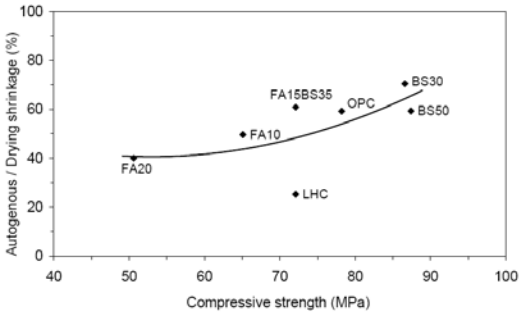

Fig. 9 Relation between the autogenous shrinkage and compressive strength

Creep

Specific creep data (strain due to creep per unit stress that cylinders are subjected to) up to 90 days are shown in Fig. 10. BS30 was not tested due to the number limit of the loading device. According to previous research, concrete with a lesser slag content in its binder gives lower specific creep (Khatri et al. 1995). Although both slag and fly ash were incorporated with FA15BS35, when FA15BS35 and BS50 were compared, they showed the same tendency as the previous research, as observed in Fig. 10. At an early age, the specific creep of concretes incorporating slag, such as BS50 and FA15BS35, was lower than that of OPC. In the long term; however, their specific creep was higher than that of OPC. In particular, BS50 had the second highest specific creep, following LHC, and the specific creep of BS50 and LHC trended upward, even at 90 days. The concretes incorporating fly ash showed higher specific creep than that of OPC. In addition, when FA10 and FA20 were compared, it appears that concrete with higher fly ash content gave higher specific creep, but this was inconsistent with other reports from the literature (Khatri et al. 1995; Sivasundaram et al. 1991). This phenomenon can be explained by noting that the age at the time of loading was 3 days. At this age, fly ash concrete has relatively low compressive strength due to its slow pozzolanic reactions. Indeed, as shown in Fig. 10,

the specific creep of FA10 and FA20 increased markedly during the first 7 days, but thereafter, increased at more slowly than any other of the concretes.

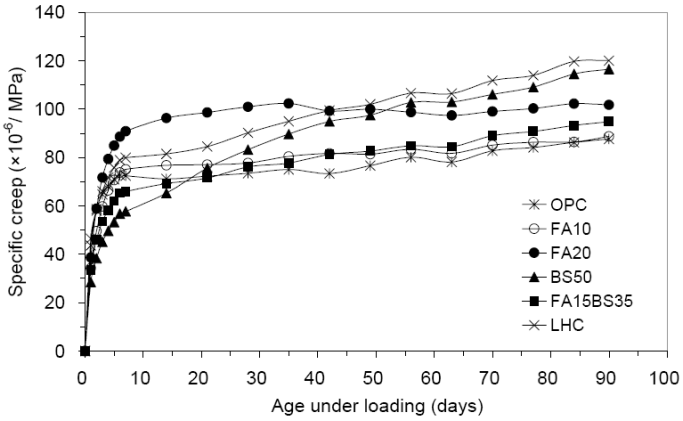

Fig. 10 Specific creep of the concretes

CONCLUSIONS

To provide information on the mix proportions, mechanical properties and durability of HSC for use in prestressed bridges, this research mainly focused on studying the effects of the type and composition of cementitious materials on the properties of HSC. Firstly, mix proportions were designed based on a number of trial mixes, taking into account early age compressive strength, workability and air content so that the developed concrete would be suitable for prestressed bridges. Based on the results of this research, the following conclusions were drawn:

1. For the ternary mixture of FA15BS35 and LHC, the highest temperature increase was much lower than that of OPC. All specimens were at similar levels at the time when the highest temperature increase was achieved.

2. Supplementary cementitious materials resulted in decreased compressive strengths at early ages. At the 28th and 56th days; however, concretes incorporating slag had higher strengths than OPC. Increase of the rate of strength of fly ash concrete after 28 days was the highest.

3. The ACI 363R-92 equation seems to provide a good prediction of the elastic modulus of HSC incorporating supplementary cementitious materials. At early ages, the percentage gain in the elastic modulus of concretes incorporating the mineral admixtures was lower than those of OPC and LHC.

4. The higher the compressive strength, the lower the tensile to compressive strength ratio. The flexural strength was found to increase with increasing compressive strength. The type and composition of cementitious material had no significant effects on the splitting tensile and flexural strengths.

5. Regardless of the type of mineral admixtures, chloride-ion permeability improved with the increasing rate of replacement. In general, the chloride migration coefficient decreased with the increasing compressive strength. However, LHC showed inferior resistance to chloride-ion, although its compressive strength was relatively high.

6. In general, and regardless of the type of mineral admixtures and replacement percentage, not

only concretes incorporating supplementary cementitious materials, but also OPC and LHC, had excellent durability factors to repeated freezing and thawing cycles. Concretes subjected to freeze–thaw cycles in CaCl2 solution had lower durability factors than in water, but the chloride solution did not significantly affect resistance to freezing and thawing of concretes with low or no replacement rates.

7. The increase in the incorporation of slag leads to increases in both autogenous and drying shrinkages of HPC. The incorporation of fly ash decreases the autogenous shrinkage, but increases the drying shrinkage in the same manner as the incorporation of slag. When both slag and fly ash are incorporated, the effect of the slag appears to dominate the shrinkage characteristic of HSC. The shrinkage characteristic of LHC is superior to that of OPC. Most of the drying shrinkage is attributed to autogenous shrinkage for HSC.

8. Concretes incorporating supplementary cementitious materials showed higher specific creep than that of OPC. When a load is applied at an early age, the specific creep of fly ash concrete increases markedly at an early age, but thereafter, increases very slowly. LHC had the highest specific creep.

NOTATION

The following symbols are used in this paper :

c_d = chloride concentration at which the color changes, N;

c_0 = *chloride concentration in the catholyte solution, N;*

D = non-steady-state migration coefficient, m^2/sec;

erf = *error function;*

F = *faraday constant, J/V·mol;*

f_c' = specified compressive strength of concrete, MPa;

L = thickness of the specimen, m;

R = gas constant, J/K·mol;

T = average value of the initial and final temperatures in the anolyte solution, K;

t = test duration, sec;

U = absolute value of the applied voltage, V;

x_d = average value of the penetration depths, m; and

z = absolute value of ion valence

REFERENCES

American Concrete Institute (ACI). (1992). “State-of-the art report on high strength concrete.” *ACI 363R-92*, Farmington Hills, Mich.

American Concrete Institute (ACI). (2005). “Building code requirements for structural concrete and commentary.” *ACI 318-05 and ACI 318R-05*, Farmington Hill, Mich.

FIP/CEB, (1990). “High strength concrete, state-of-the-art report.” Bulletin d’Information No. 197, 61 pp.

Hueste, M. B. D., Chompreda, P., Trejo, D., Cline, D. B. H., and Keating, P. B. (2004). “Mechanical properties of high-strength concrete for prestressed members.” *ACI Struct. J.*, 101(4), 457-466.

Japan Concrete Institute Technical Committee on Autogenous Shrinkage of Concrete (1999). “Committee report-autogenous shrinkage of concrete.” E & FN Spon, London and New York.

Khatri, R. P., Sirivivatnanon, V., and Gross, W. (1995). “Effect of different supplementary cementitious materials on mechanical properties of high performance concrete.” *Cem. Concr. Res.*, 25(1), 209-220.

Leng, F., Feng, N., and Lu, X. (2000). “An Experimental study on the properties of resistance to diffusion of chloride ions of fly ash and blast furnace slag concrete.” *Cem. Concr. Res.*, 30(6), 989-992.

Metha, P. K., and Monteiro, P. J. M. (1993). *Concrete: Structure, Properties, and Materials*, 2nd Ed., Prentice-Hall, New Jersey.

Mokhtarzadeh, A., Kriesel, R., French, C., and Snyder, M. (1995). “Mechanical properties and durability of high-strength concrete for prestressed bridge girders.” *Transport. Res. Rec.*, n1478, 20-29.

Mu, R., Miao, C., Luo, X., and Sun, W. (2002). “Combined deterioration of concrete subjected to loading, freeze-thaw cycles and chloride salt attack.” *Mag. Concr. Res.*, 54(3), 175-180.

Neville, A. M. (1995). *Properties of Concrete*, 4th Ed., Longman Group Ltd, London.

Russell, B. W. (1994). “Impact of high-strength concrete on the design and construction of pretensioned girder bridges.” *PCI J.*, 39(4), 76-89.

Saak, A. W., Jennings, H. M., and Shah, S. P. (2004). “A generalized approach for the determination of yield stress by slump and slump flow.” *Cem. Concr. Res.*, 34(3), 363-371.

Sivasundaram, V., Carette, G. G., and Malhotra, V. M. (1991). “Mechanical properties, creep, and resistance to diffusion of chloride ions of concretes incorporating high volumes of ASTM Class F fly ashes from seven different sources.” *ACI Mater J.*, 88(4) 407-416.

Tazawa, E., and Miyazawa, S. (1995). “Influence of cement and admixture on autogenous shrinkage of cement paste.” *Cem. Concr. Res.*, 25(2), 281-287.

Toutanji, H., Delatte, N., Aggoun, S., Duval, R., and Danson, A. (2004). “Effect of supplementary cementitious materials on the compressive strength and durability of short-term cured concrete.” *Cem. Concr. Res.*, 34(2), 311-319.

Yazdani, N., Bergin, M., and Majtaba, G. (2000). “Effect of pumping on properties of bridge concrete.” *J. Mater. Civ. Eng.*, 12(3), 212-219.